DTU Library

Unprecedented strength in pure iron via high-pressure induced nanotwinned martensite

Zhang, Hongwang; Wang, Yuhui; Peng, Yan; Zhu, Pinwen; Liu, Jianhua; Feng, Zongqiang; Wu, Guilin; Huang, Xiaoxu

Unprecedented strength in pure iron via high-pressure induced nanotwinned martensite

Hongwang Zhang, Yuhui Wang, Yan Peng, Pinwen Zhu, Jianhua Liu, Zongqiang Feng, Guilin Wu & Xiaoxu Huang

Published online: 07 May 2019.

Submit your article to this journal

Article views: 284

View Crossmark data

MATERIALS
RESEARCH LETTERS

Taylor & Francis
Taylor & Francis Group

ORIGINAL REPORT

🔓 OPEN ACCESS   Check for updates

Unprecedented strength in pure iron via high-pressure induced nanotwinned martensite

Hongwang Zhang[a,b]*, Yuhui Wang[a,b]*, Yan Peng[a], Pinwen Zhu[c], Jianhua Liu[b], Zongqiang Feng[d], Guilin Wu[d] and Xiaoxu Huang[d,e]*

[a]National Engineering Research Center for Equipment and Technology of Cold Strip Rolling, College of Mechanical Engineering, Yanshan University, Qinhuangdao, People's Republic of China; [b]State Key Laboratory of Metastable Materials Science and Technology, Yanshan University, Qinhuangdao, People's Republic of China; [c]State Key Laboratory of Superhard Materials, College of Physics, Jilin University, Changchun, China; [d]College of Materials Science and Engineering, Chongqing University, Chongqing, People's Republic of China; [e]Department of Mechanical Engineering, Technical University of Denmark, Lyngby, Denmark
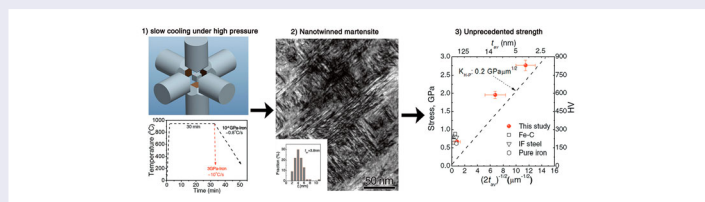
ABSTRACT

Martensitic transformation can easily induce a maximum hardness value of 800–900 HV (Vickers hardness) for steels with carbon contents of 0.6 wt.% and above. However, the occurrence of martensitic transformation in pure iron requires exceptionally high cooling rates (10^5–10^6°C/s), and the maximum achievable hardness is only about 150 HV. Here we report an extreme hardness of 830 HV in pure iron obtained through high pressure induced martensitic transformation at a rather slow cooling rate of just 10°C/s. This unprecedented strength originates from the formation of twin-related martensitic laths with an average thickness of 3.8 nm.

IMPACT STATEMENT

Slow cooling of pure iron under high pressure induces martensitic transformation, producing nanotwinned martensite with unprecedented strength.

1. Introduction

Iron has played an important role in the progress of human civilization [1]. It is well-known that pure iron is very soft (< 100 HV) and can be hardened by making it into steels through adding carbon and other alloying elements. The maximum hardening in iron and steels is achieved by martensitic transformation up to 800–900 HV [2], i.e. a diffusionless and shear displacive transformation that changes the high temperature austenite form to fine scale martensite containing a high density of lattice defects. The hardening is mainly originated from three mechanisms: (i) solid solution strengthening by supersaturation of carbon atoms inside the Fe lattice [3], (ii) dislocation strengthening that is proportional to the square root of dislocation density [4], and (iii) Hall-Petch strengthening that is proportional to the reciprocal of the square root of grain size (spacing between boundaries) [5, 6]. However, with decreasing carbon content, the temperature at which the martensitic transformation begins under conventional cooling rates (M_s point) increases [7, 8]. Accordingly, the martensitic M_s point for pure iron is so high (> 700°C) that extremely fast cooling of 10^5–10^6°C/s is needed for the martensitic transformation to occur. Moreover, the

transformed martensite has insignificant lattice supersaturation, a relatively low dislocation density ($10^{14} m^{-2}$) and a coarse boundary spacing (~ 500 nm), and hence a hardness of only 150 HV [9].

As a thermodynamic variable independent of chemical composition, the pressure (P) can enhance the driving force for martensitic transformation and decrease the M_s point by providing extra work to increase the change in Gibbs free energy [10], and consequently, tune the substructure that controls the martensite strength. A previous investigation [11] demonstrated that application of a pressure of 3–5 GPa causes the martensitic substructure in low carbon steels to be dominated by nanoscale internal twins of the type that are commonly found in martensite of high carbon steels transformed under atmospheric pressure. A recent study also showed that quenching under a pressure of 5 GPa induces lath martensite in an interstitial-free (IF) steel that otherwise does not form martensite during quenching under atmospheric pressure [12]. Herein, pure iron samples were subjected to a heating and cooling cycle under high pressure, leading to the formation of martensite. The martensite formed comprises nanoscale laths, with each lath a crystallographically equivalent variant, and adjacent variants related by a twin misorientation ($60°/<111>$). This nanoscale martensite exhibits an ultrahigh hardness of 830 HV. This discovery highlights an incredible hardening by martensitic transformation in pure iron.

2. Experimental methods

A commercial high purity iron (0.0021 wt.%C, 0.012 wt.% Mn, 0.0064 wt.% P, 0.0028 wt.% S and Fe the balance) was subjected to heating and cooling under either atmospheric pressure (10^{-4} GPa; the corresponding sample is referred to as 10^{-4} GPa-iron) or high pressures of 1, 2, and 3 GPa (1, 2, and 3 GPa-iron). As schematically illustrated in Figure 1(a), a hexahedron pressure equipment was used to generate high pressure by equally compressing the six sides of a cubic sample ($5 \times 5 \times 5$ mm^3) using a CS-I B and SPD-6-600 hexahedral multi-anvil unit. The sample assembly consisted of heater, insulator, and pressure transmitting medium. The temperature was measured with K-type thermocouples, and the pressure was estimated from previously obtained calibration curves for the multi-anvil high pressure apparatus [13, 14]. The sample was gradually compressed to the desired pressure at room temperature and then was heated at 1°C/s to the desired temperature referring the Fe-C phase diagram under hydrostatic and atmospheric pressure [15], namely, 300, 600, 720, 780, 880, 950 and 1050°C, respectively. As shown by Figure 1(b), the duration holding at each setting temperature was 1800 s,
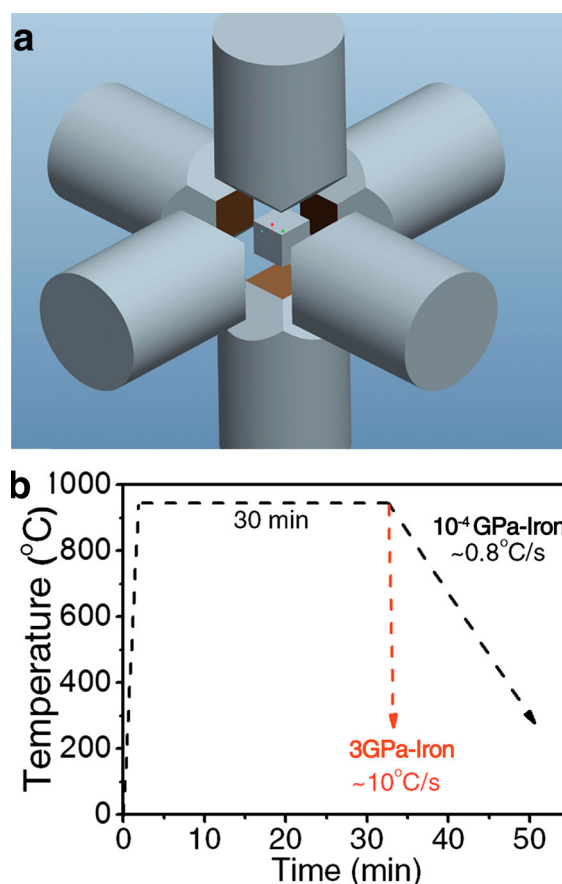
Figure 1. (a) Schematic illustration of the hexahedron pressure facility. (b) The heating and cooling cycle under different pressure.

followed by cooling to ambient temperature in 90 s by switching off the power and then slowly decompressed. The cooling rate from 950°C to ambient temperature was roughly 10°C/s. Heating and cooling under atmospheric pressure were performed in a vacuum furnace. The sample was heated to 950°C in 15 s and held for 1800 s, followed by furnace cooling to ambient temperature in 1200 s, corresponding to a cooling rate of ~ 0.8°C/s.

The microstructure of the final products after heating and cooling cycle under pressure was characterized by optical microscopy, scanning electron microscopy, electron backscatter diffraction (EBSD), transmission electron microscopy (TEM) and high resolution TEM (HRTEM). TEM samples were made by focused ion beam (FIB) milling with an FEI SHNNNP Scios dual-beam facility, from the area close to the corresponding hardness indentations. TEM and HRTEM observations were performed in the FEI Talos 200X TEM and JEM 2100 TEM operated at an accelerating voltage of 200 kV. The thickness of parallel laths was measured on the TEM micrographs along lines that are perpendicular to the laths.
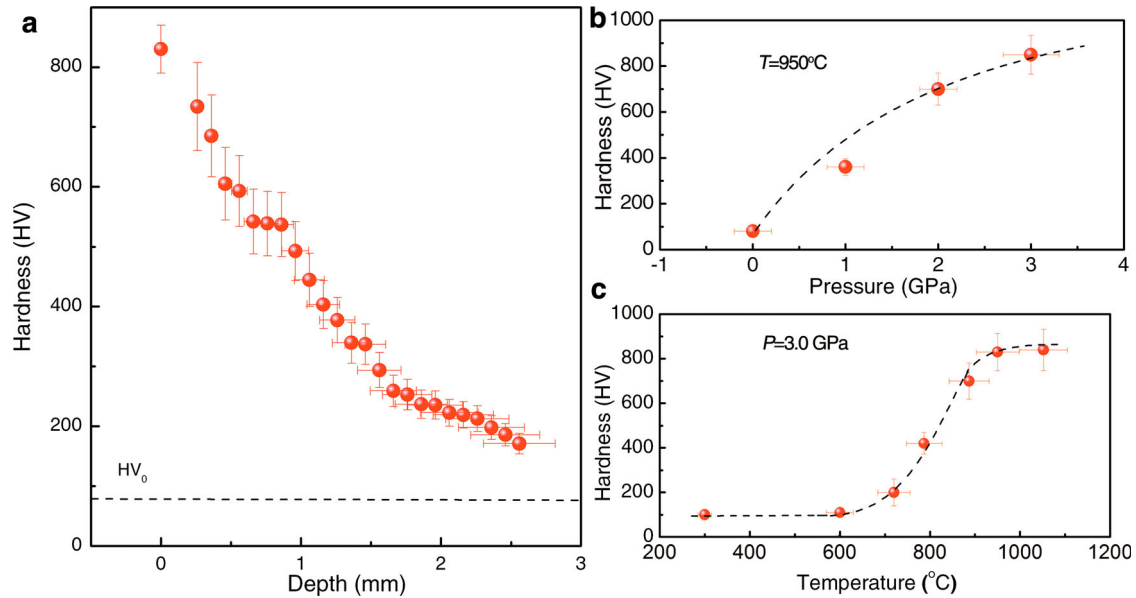
Figure 2. Variation of hardness as a function of depth (a), the applied pressure at a holding temperature of 950°C (b) and the holding temperature under 3 GPa **c** for pure iron sample.

Vickers hardness was measured on a Quness 10A+ microhardness tester with a load of 0.98 N and a duration of 10 s. Each hardness value was averaged over at least ten measurements.

3. Results

It is surprising that remarkable hardening was obtained in pure iron after the heating and cooling cycle under high pressures, as shown in Figure 2. The 3 GPa-iron sample exhibited an unprecedented ultrahigh hardness of 830 HV for holding temperatures above 950°C. This hardness value is one order of magnitude higher than that of the starting material (80 HV). This value is 5–6 times higher than that of pure iron cooled under atmospheric pressure at 10^5–10^{6}°C/s (150 HV) [9] and is comparable to that (800 ∼ 900 HV) of martensite in carbon steels containing > 0.6 wt.% C [3]. The hardening varies with depth and depends upon the holding temperature and applied pressure. From Figure 2(a), the hardness of 3 GPa-iron decreases continuously to 400 HV at a depth of 1 mm, and then reaches 200 HV in the sample center. With decreasing holding temperature, the hardening becomes increasingly less significant and eventually no hardening is observed for holding temperatures below 720°C, as shown in Figure 2(b). At a holding temperature of 950°C, the hardness decreases to 700 and 400 HV as the pressure is reduced to 2 and 1 GPa, respectively, as shown in Figure 2(c).

All processed pure iron samples have the body-centered cubic (bcc) structure, which was verified by X-ray diffraction. Optical microscopy observations showed
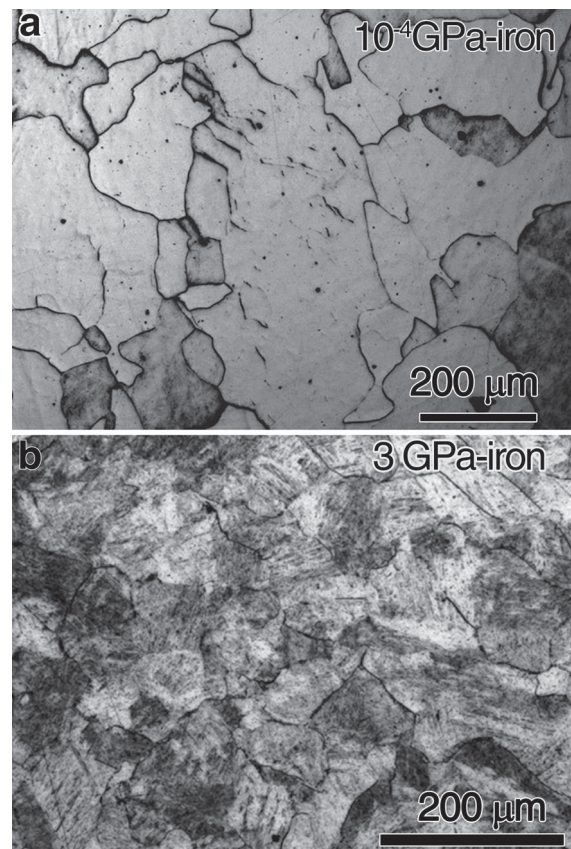
Figure 3. The optical micrographs of the 10^{-4}GPa-iron (a) and the 3GPa-iron with a holding temperature of 950°C (b).

that the bcc phases in the high pressure samples with holding temperatures below 720°C are characterized by coarse and irregular grains with clean interiors, like
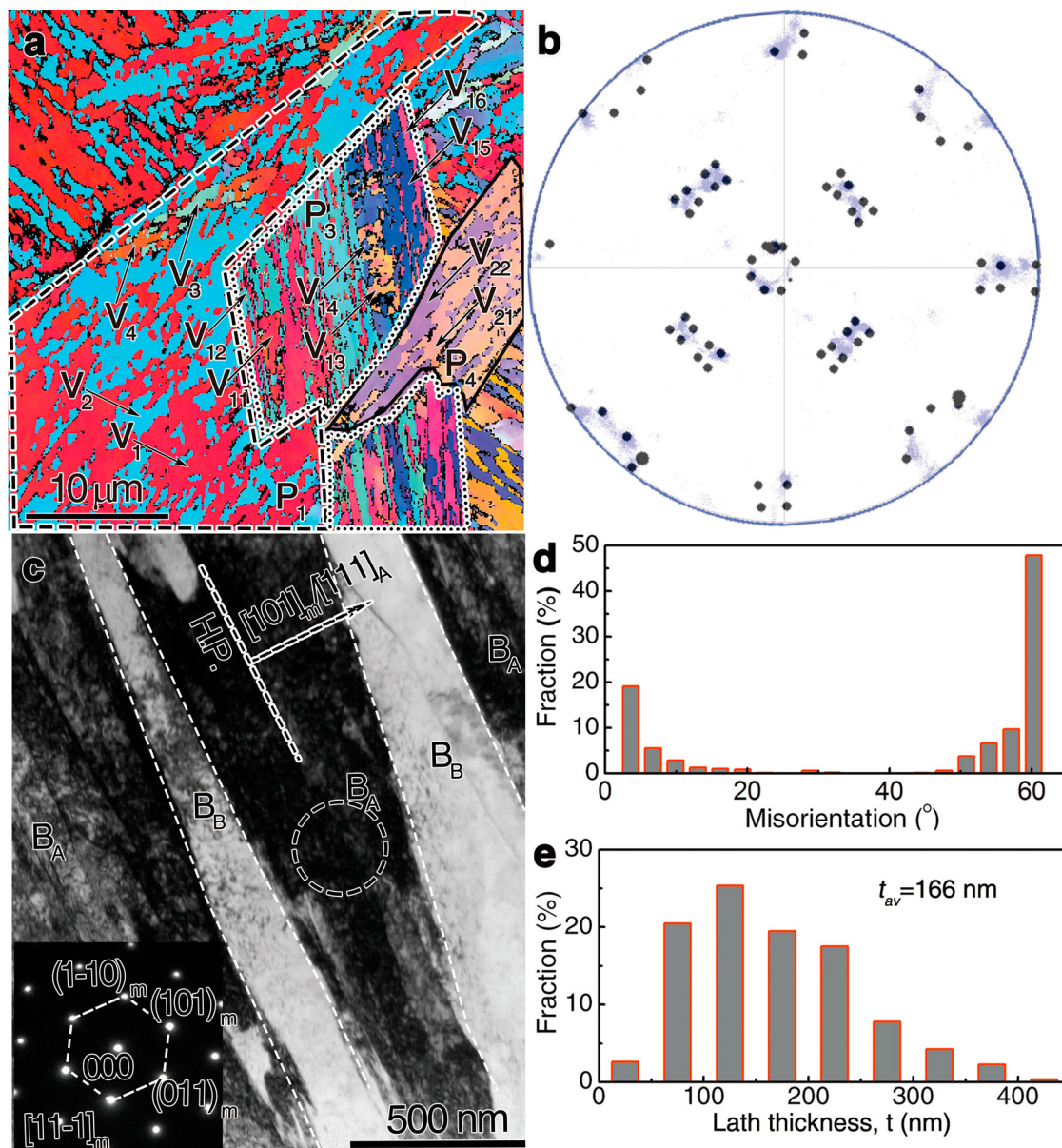
Figure 4. Structural overview of the center of 3GPa-iron at a holding temperature of 950°C: (a) EBSD inverse pole figure image of a packet–block. (b) Experimental (blue clouds) and theoretical (black dots) orientation distributions in the {001} pole figure. (c) TEM observation. (d) Distribution of boundary misorientations and (e) Thickness of the martensite laths. The variant pairs V_x in (a) were indexed according to [16], and the boundaries enclosing the three packets P_1, P_3, and P_4 are marked by dashed, dotted, and full lines, respectively.

that in the 10^{-4}GPa-iron shown in Figure 3(a). As the holding temperature exceeds 720°C, substructures are observed inside the grain interiors of the high pressure samples (Figure 3(b)), resembling the hierarchical packet–block–lath structure of the lath martensite observed in IF steel or low carbon steels [16]. Notably, a gradient structure was present inside the cubic sample, showing lath martensite with different structural scales.

The lath martensite at the center of 3 GPa-iron with a holding temperature of 950°C has a relatively coarse substructure, as demonstrated by the EBSD characterization (Figure 4(a)). Three packets of several to tens

of micrometers in width, labeled P_1, P_3 and P_4 in the figure, are seen within the observed area of a grain. Each packet contains regions of similar colors, representing blocks with roughly the same crystal orientation. The orientation relationship (O.R.) between the martensite (m) and the parent austenite (A) follows the Kurdjumov–Sachs (K–S) OR [17], $\{111\}_A//\{011\}_m$ and $<110>_A//<111>_m$, which is revealed by the good agreement between the experimentally measured martensite orientations (blue cloud) and those of the 24 K–S variants (black solid circle) in the {001} pole figure shown in Figure 4(b). Each block was observed to contain

only one martensitic variant, and adjacent variants in the same packet show a twin misorientation with an axis/angle pair of $<110>/70.5°$ or $<111>/60°$, which corresponds to the misorientation for twin-related variants [16]. These misorientations lead to the peak around 60° in the histogram of misorientation distribution in Figure 4(d). TEM reveals that each block in Figure 4(c) contained laths with an average thickness of 166 nm and predominantly low misorientation angles (Figure 4(e)). The habit plane of the martensite laths was close to $(101)_m$ and $(111)_A$, which is in agreement with that of typical lath martensite in IF steels and low carbon steels [18].

Martensite induced close to the sample surface has fine-scale substructure, with a K–S O.R. between austenite and martensite, and $(111)_A$-type habit plane (deviation of 5.5°), as shown in Figure 5(a). The packets are reduced in size to tens of nanometers in width (for instance 40–50 nm for packets d and e), and the block thickness ranges from 2 to 10 nm with an average of 3.8 nm (Figure 5(b,f)). This length scale is 1–2 orders of magnitude smaller than that of the coarse lath martensite (~ 166 nm) in the sample center and is even smaller than that (5–10 nm) of high carbon martensite [3]. Each block corresponds to a single variant that is twin-related to adjacent blocks in the same packet (variant pair: V_1–V_2 and V_{15}–V_{16}), as evident from the mirror symmetric bcc [110] diffraction patterns (Figure 5(c)). Based on the high resolution TEM images (Figure 5(d,e)), the (1–10) crystallographic planes (solid lines) from twin-related variants are mirror symmetric. Such a martensitic structure is referred to as nanotwinned martensite hereafter in this paper.

4. Discussion

Here, the martensitic transformation could proceed under slow cooling as high pressure was applied to raise the driving force by increasing the change in Gibbs free energy [10], to suppress atomic diffusion [21], and to shift the continuous cooling transformation curve rightward [22]. Previous investigations [11, 23] reported that an application of 3–5 GPa pressure causes the martensitic transformation to proceed at a cooling rate of 100°C/s in Fe–C and Fe–Cr alloys; a recent study [12] even demonstrated that a martensitic structure could be formed in an IF steel cooled under a pressure of 5 GPa at 8°C/s. The present study shows that lath martensite in pure iron can be induced to form under a pressure of 1–3 GPa at a cooling rate of 10°C/s which is 4–5 orders of magnitude slower than that required for martensitic transformation under atmospheric pressure. The lath martensite has the typical packet–block–lath structure holding the

K–S O.R. with the parent austenite and $(111)_A$-type habit planes, as observed in low carbon steels [18]. However, it is surprising to observe that the adjacent blocks in the same packet comprise twin-related variants, and the block sizes are substantially reduced to the nanoscale with increasing pressure. According to the phenomenological theory of martensite crystallography, approximate twin-related variants are more efficient in accommodating transformation strain than other pairs [24]. Moreover twin-related variant selection is enhanced as more carbon is added to decrease the M_s point [25, 26], which is accompanied by substantially reduced block and packet sizes due to the harder austenite against deformation [27]. Theoretically, the application of every 1 GPa pressure decreases the M_s point by 82 K [11], whereas a 100 K temperature drop strengthens austenite at high temperatures by 18 MPa [28]. In addition, the flow stress (σ_y) of a material subjected to high pressure is linearly related to the pressure amplitude (P) ($\sigma_y = (1 + 3kP) \sigma_0)$, where σ_0 is the flow stress at atmospheric pressure, and k is the pressure coefficient; for steels, $k = 0.02$ [29]. Consequently, the present pressure of 3 GPa may induce M_s point drop of 246 K, equivalent to the addition of 0.77 wt% C, following $\Delta M_s = 320$ K/wt %C [28], and an austenite strengthening by 53 MPa. These changes facilitate the formation of nanoscale twin-related laths. However, such martensite was neither observed in pure iron cooled under 5–7 GPa pressure that was introduced by piston-cylinder type high pressure apparatus [11] nor in IF steel cooled under 5 GPa pressure that was produced by the constrained volume expansion of NaCl in melting [12]. This difference may point to an effect of the procedure by which the high pressure is generated on the martensitic transformation. The current procedure of applying high pressure by equally pressing on the six sides of a cubic sample with hexahedron pressure equipment may restrict the volume change more effectively than other methods, rendering the occurrence of martensitic transformation at relatively low pressures.

The present hardening of pure iron by one order's of magnitude highlights the significance of martensitic hardening via structural refinement. When the double lath thickness value ($2t_{av}$) [21, 30] is viewed as the slip length (d) for the H–P relationship ($\Delta\sigma = K_{HP}d^{-1/2}$, where $\Delta\sigma$ is the strengthening (ΔHV/3), K_{HP} is the H–P coefficient), a K_{HP} of 0.2 GPaμm$^{1/2}$ was obtained as shown in Figure 5(g), comparable to that for a polycrystalline pure iron [19]. However, the present data points and the previously reported ones [9, 12, 20] lie above the H–P line for the polycrystalline pure iron (dashed line in Figure 5(g)), showing an extra strengthening of 200–400 MPa that may stem from the dislocations present in the martensite.
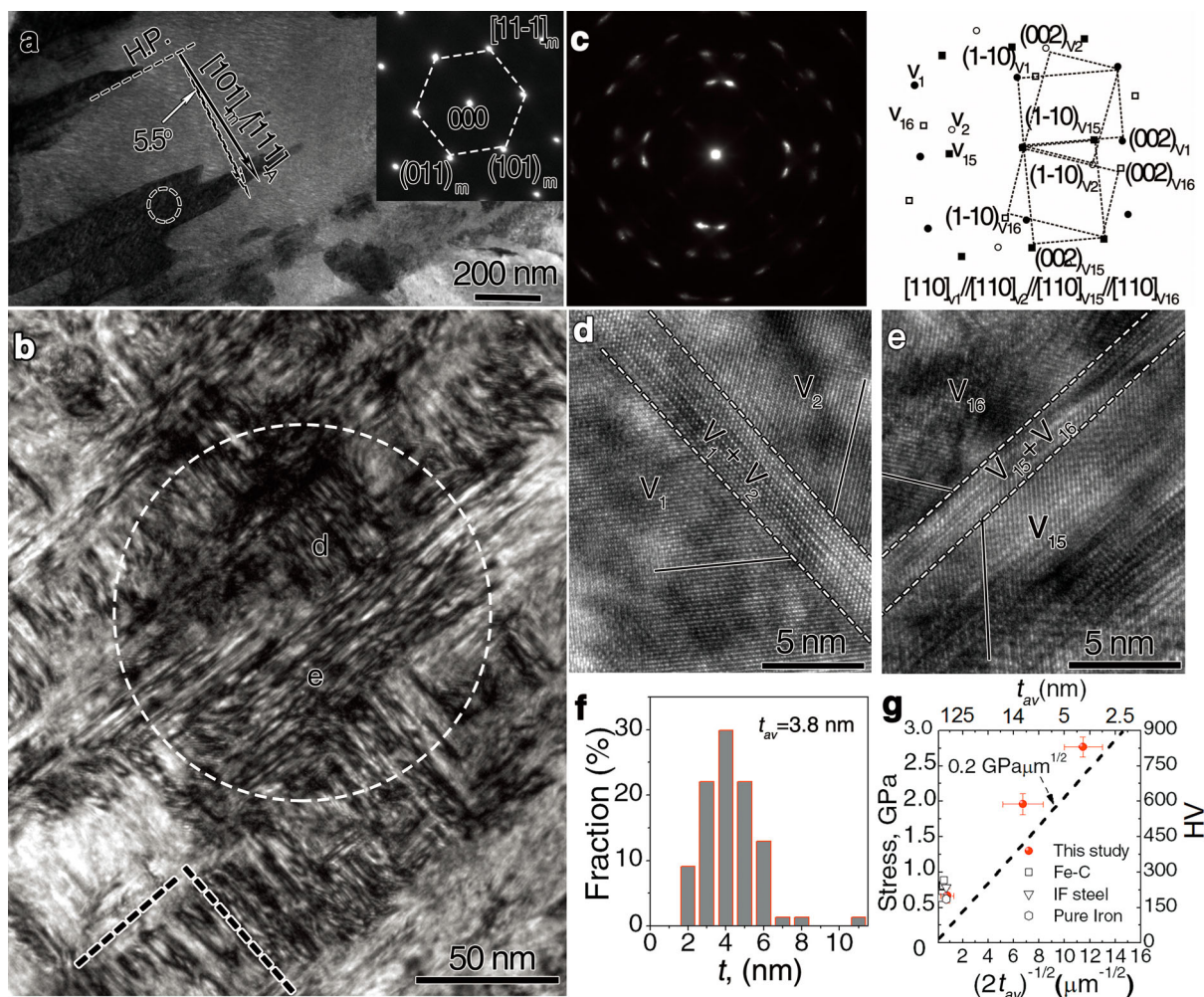
Figure 5. Structural overview of the surface of 3GPa-iron at a holding temperature of 950°C: (a, b) TEM observations. (c) SAED pattern and the indexed sketch map. (d, e) High resolution TEM images. (f) Histogram of the lath thickness, d_{lath}, of the twin related variants. (g) Hall–Petch (H–P) plot. Dashed line indicates the H-P plot of high pure iron (1 month annealing at 850°C in wet hydrogen) [19]. Literature data on the martensite of pure iron [9], IF steel [12] and Fe–C [20] were inserted for comparison. The white circle in (b) marks the area where the SAED pattern in (c) was obtained.

5. Conclusion

Martensitic transformation was induced in pure iron under high pressure with a slow cooling of 10°C/s. The martensite was characterized by twin-related laths with an average thickness of 3.8 nm. The martensitic transformation resulted in an unprecedented strengthening by a factor over 10. These new findings may expand the processing space for tuning the structure and strength of iron and, showing great technical importance for a wide range of industrial applications.

Disclosure statement

No potential conflict of interest was reported by the authors.

Acknowledgments

We thank K. Lu of Institute of Metal Research, Chinese Academy of Sciences, Y.J. Tian, D.L. Yu, Z.S. Zhao, H.Y. Gou of Yanshan University, N. Hansen and D. Juul Jensen of Technical University of Denmark, A. Godfrey from Tsinghua University, for helpful discussions. We thank T.L. Huang of Chongqing University, and G.H. Fan of Harbin Institute of Technology for their help with data collection and analysis.

Funding

This work was supported by the Project of Hundred Outstanding Creative Talents in the Universities in Hebei Province, China, the Project Program of Heavy Machinery Collaborative Innovation Center, the National Natural Science Foundation of China [grant numbers 51171182, 51871194] and the State Key Research and Development Program of MOST of China [grant number 2016YFB0700400].

References

[1] Wertime TA. Man's first Encounters with metallurgy. Science. 1964;146:1257–1268.

[2] Maddin R. In: Olson GB, Owen WS, editor. Martensite. Materials Park, OH: ASM International; 1992. p. 11.

[3] Krauss G. Martensite in steel: strength and structure. Mater Sci Eng A. 1999;273–275:40–57.

[4] Taylor GI. The mechanism of plastic deformation of crystals I. Theoretical. Proc Roy Soc. 1934;A145:405–415.

[5] Hall EO. The deformation and ageing of mild steel: III discussion of results. Proc Phys Soc Lond B. 1951;64:745–753.

[6] Petch NJ. The cleavage strength of polycrystals. J Iron Steel Inst. 1953;174:25–28.

[7] Morito S, Nishikawa J, Maki T. Dislocation density within lath martensite in Fe-C and Fe-Ni alloys. ISIJ Int. 2003;43:1475–1477.

[8] Kelly PM, Nutting J. The martensite transformation in carbon steels. J Proc Roy Soc. 1960;A 259:45–58.

[9] Speich GR, Szirmae A, Fisher RM. A laser heating device for metallographic studies. Proc Symp Electr Metall ASTM Spec. Publication No. 396, 1966; 97, Philadelphia.

[10] Patel JR, Cohen M. Criterion for the action of applied stressing the martensitic transformation. Acta Metall. 1953;1:531–538.

[11] Vyhnal RF, Radcliffe SV. Effect of pressure on the structure of iron-carbon martensites. Acta Metal. 1967;15: 1475–1488.

[12] Kang JY, Kim SC, Oh JO, et al. Martensite in interstitial-free steel obtained by ultra-high pressure. Scripta Mater. 2012;66:45–48.

[13] Han QG, Yang WK, Zhu PW, et al. Design and performance of tapered cubic anvil used for achieving higher pressure and larger sample cell. Rev Sci Instrum. 2013;84:073902-1-5.

[14] Yuan B, Tao Q, Zhao XP, et al. In situ measurement of electrical resistivity and Seebeck coefficient simultaneously at high temperature and high pressure. Rev Sci Instrum. 2014;85:013904-1-4.

[15] Hillard JE. Iron-carbon phase diagram: isobaric sections of the eutectoid region at 35, 50, and 65 kilobars. Trans Metall Soc AIME. 1963;227:429–438.

[16] Morito S, Huang X, Furuhara T, et al. The morphology and crystallography of lath martensite in alloy steels. Acta Mater. 2006;54:5323–5331.

[17] Kurdjumov G, Sachs G. Über der mechanismus der stahlhärtung (On the mechanism of hardening of steel). Z Phys. 1930;64:325–343.

[18] Maki T., Pereloma E, Edmonds D.V. 2012. Phase Transformations in Steels. Woodhead, Cambridge; 2012, p. 34.

[19] Armstrong R, Codd I, Douthwaite RM, et al. The plastic deformation of polycrystalline aggregates. Philos Mag. 1962;7:45–58.

[20] Morito S, Yoshida H, Maki T, et al. Effect of block size on the strength of lath martensite in low carbon steels. Mater Sci Eng A. 2006;438–440:237–240.

[21] Radcliffe SV, Schatz M. The effect of high pressure on the martensitic reaction in iron-carbon alloys. Acta Metall. 1962;10:201–207.

[22] Kakeshita T, Kuroiwa K. Effects of hydrostatic pressure on martensitic transformation. Mater Trans JIM. 1997;38:668–681.

[23] Pascover JS, Radcliffe SV. Effects of pressure on phase equilibrium and transformation in the Fe-Cr system. Acta Mater. 1969;17:321–338.

[24] Kelly PM. Crystallography of lath martensite in steels. Mater Trans JIM. 1992;33:235–242.

[25] Stormvinter A, Miyamoto G, Furuhara T, et al. Effect of carbon content on variant pairing of martensite in Fe-C alloys. Acta Mater. 2012;60:7265–7274.

[26] Takayama N, Miyamoto G, Furuhara T. Effects of transformation temperature on variant pairing of bainitic ferrite in low carbon steel. Acta Mater. 2012;60:2384–2396.

[27] Morito S, Tanaka H, Konishi R, et al. The morphology and crystallography of lath martensite in Fe-C alloys. Acta Mater. 2003;51:1789–1799.

[28] Greninger AB. The martensite thermal arrest in iron-carbon alloys and plain carbon steels. Trans ASM. 1942;30:1–25.

[29] Spitzig WA, Richmond O. The effect of pressure on the flow stress of metals. Acta Metall. 1984;32:457–463.

[30] Hughes DA, Hansen N. Microstructure and strength of nickel at large strains. Acta Mater. 2000;48:2985–3004.